# Marriage of an N-Fused and a Regular Porphyrin in a Cofacial Ligand System

Christoph Schissler, Erik K. Schneider, Michael Rotter, Silke Notter, Carsten Geier, Patrick Weis, Manfred M. Kappes,* and Stefan Bräse*

**ABSTRACT:** We present a straightforward synthetic route which allows cofacial stacking of N-fused porphyrins and regular porphyrins via an o-substituted phenylene linker. The protocol comprises a crucial Suzuki−Miyaura cross-coupling reaction to introduce the phenyl moiety at the tri-pentacyclic ring of the N-fused porphyrin, paving the way to the first arrangement that is capable of holding an N-fused porphyrin and a regular porphyrin in spatial proximity. The ligand system was obtained with a 0.77% yield in five steps, starting from pyrrole and benzaldehyde. The dimeric ligand was investigated for further insights into sterical properties, employing inter alia ion-mobility spectrometry, DFT calculations, and metal coordination reactions. The molecular species were characterized by $^{1}$H NMR, UV−vis, IR, high-resolution mass spectrometry, and trapped ion-mobility measurements. The latter suggests that the ligand system can stabilize two atoms of the same metal in different oxidation states, such as in an Mn(I)Mn(III) complex.

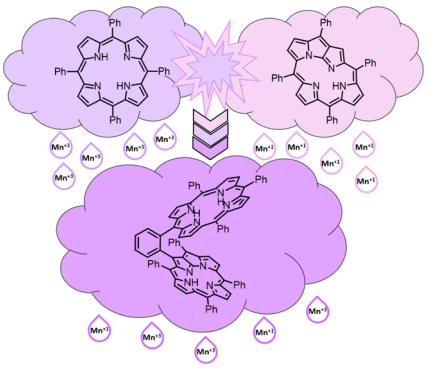

## INTRODUCTION

Porphyrins rank among the most widespread macrocycles in nature and traditionally belong to the best-explored compounds in chemistry.[1] Nevertheless, the structural versatility of porphyrinoids in terms of rearranged and twisted conformations has only been addressed in comparatively recent times.

By fusing two adjacent pyrrole rings in the porphyrinoid scaffold, as displayed in N-fused porphyrins (NFP), a decrease in the HOMO−LUMO band gap is caused without increasing the number of $\pi$-electrons. This way, optical properties are affected while maintaining an 18 $\pi$-electron system. Compared to regular porphyrin structures, significant bathochromic shifts appear, and the Q-band absorptions of certain NFP metal complexes can even extend beyond 1000 nm.[2] Additionally, NFP exhibit fluorescence in the NIR region with large Stokes shifts. Consequently, they are of interest for applications in optical communication, biosensing probes, and photovoltaics.[3]

NFP can function as a mono-negative tridentate ligand for metal ions—comparable to cyclopentadienyl or tris(pyrazolyl)-borate. The corresponding three nitrogen atoms are arranged in a compact and triangular structure with N−N distances <3 Å.[4] Thus, three of the four nitrogen atoms within the macrocyclic skeleton can tightly coordinate a metal center. Complexes of NFPs with various atomic cations can be grouped into "in-plane" and "atop" coordination types. Due to the tri-pentacyclic rings, only ions with comparatively small ionic radii can be incorporated into the NFP plane, as is the case for the B(III) complexes reported by Latos-Grażyński et al.[5] By contrast, P(V),[6] Mn(I),[7] W(VI),[8] Re(I),[9,10] Rh(I),[11] and Ir(I)[11] all coordinate above the NFPs' plane. This provides enough space for various ancillary ligands—a feature which cannot be realized in regular, in-plane porphyrin−metal complexes of 3d metals. Heavier metals also coordinate above the center of regular porphyrins and/or with additional ancillary ligands. Some examples are Sn,[12] Bi[13],[3], Ru, Os,[14] Re[15],[5], Pb,[16] and different lanthanides.[17−19]

Linus Pauling and Melvin Calvin were the first to propose the so-called "isoporphyrins" with "extroverted pyrrole rings" in the 1950s—hypothetical structures that were independently discovered 50 years later by the groups of Furuta[20] and Latos-Grażyński.[21] These molecules became later known as "N-confused porphyrins". The broken-symmetry N-confused porphyrin was the key to synthesizing NFPs. In contrast to regular porphyrins, N-confused porphyrins exhibit diminished intramolecular hydrogen bonds and aromaticity, enabling the necessary pyrrole ring flipping at ambient temperature.[22] After introducing a leaving group at the 2′ position of the twisted pyrrole, a smooth, base-catalyzed nucleophilic intramolecular attack can yield the respective NFP. Senge nicely reviewed the synthetic breakthrough that paved the way toward NFP complexes in 2011.[23]

As our consortium had recently developed synthetic protocols for cofacially connecting porphyrin dimers[24] and trimers,[25] we aimed for an expanded range of applications, namely the novel dimeric ligand system containing an NFP and a regular porphyrin. Below, we demonstrate a corresponding synthesis protocol and show that this new ligand system can stabilize two manganese atoms in two different oxidation states, holding them in spatial proximity via a cofacial arrangement. Such systems are of application interest in the context of their cooperative properties, e.g., as homogeneous catalysts.

## RESULTS AND DISCUSSION

**Ligand Synthesis.** NFPs were synthesized from N-confused porphyrins. The latter can be made much like normal porphyrins, except that the acid catalyst TFA/$BF_3$·$OEt_2$ gets substituted for methanesulfonic acid ($MeSO_3H$). Following the procedure developed by Lindsey et al., pyrrole (**1**) was stirred together with benzaldehyde (PhCHO) in the presence of $MeSO_3H$ at room temperature for 30 min in the absence of light to afford **2** in 29% yield (Scheme 1).[26]

**Scheme 1. Synthesis of the N-Confused-Tetraphenylporphyrin 2**

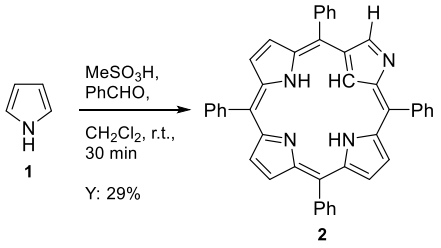


The $^1$H NMR spectrum of **2** shows a singlet at 8.77 ppm that can be assigned to the outer proton of the twisted pyrrole ring. Moreover, the high-field region of the corresponding spectrum exhibits a broad singlet at −2.43 ppm, which can be assigned to the NH protons, and a slightly broadened singlet at −4.99 ppm, which can be attributed to the interior CH proton. UV−vis absorption bands in $CH_2Cl_2$ compared to regular tetraphenylporphyrin (TPP) are red-shifted. The Soret-band of **2** lies at 439 nm, and the Q-bands show maxima at 541, 582, and 726 nm.[27,28]

The N-confused porphyrin **2** was stirred for 5 min with N-bromosuccinimide (NBS) (2.30 equiv) to obtain the unstable dibromo-N-confused porphyrin **3** as an intermediate (Scheme 2). The crude product was filtered through a short pad of silica gel and redissolved in pyridine. To promote the fusion to a [5,5,5] fused tri-pentacyclic ring, the pyridine-solution of **3** mentioned above was stirred at r.t. for 1 h, and the bromo-NFP **4** was obtained in 55% yield over two steps from **2**.

$^1$H NMR spectroscopy of **4** showed doublets in the 7−8 ppm region with increased coupling constants ($J$ = 5.1 Hz) compared to the regular porphyrin scaffold ($J$ = 4.6 Hz for diphenylporphyrin), caused by its slightly bent structure.[28]

Subsequently, **4** was subjected to a Suzuki−Miyaura cross-coupling reaction to yield the formyl-phenyl-NFP **5** in 22% yield (Scheme 3).

Best results were obtained under the standard conditions used to generate formyl-phenyl derivatives of common porphyrins, consisting of the use of 2-formylphenylboronic acid, $Pd(PPh_3)_4$, and $K_3PO_4$ in degassed THF, but at an

**Scheme 2. Synthesis of the Doubly Brominated N-Confused Porphyrin 3 and the Subsequent Base-Catalyzed Intramolecular Nucleophilic Attack to Yield the Bromo-N-Fused Porphyrin 4; (a) NBS, $CH_2Cl_2$, r.t., 5 min; (b) Pyridine, r.t., 1 h, Y: 55% (2 Steps)**

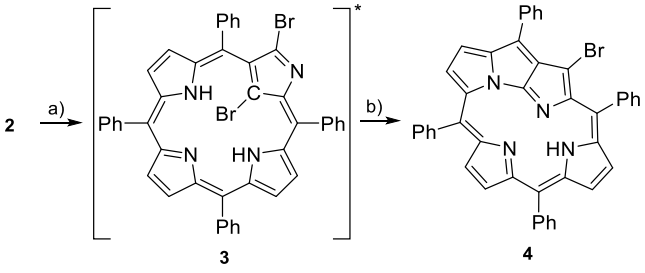


**Scheme 3. Pd-Catalyzed Suzuki−Miyaura Cross-Coupling Reaction to Yield the Formyl-Phenyl-N-Fused Porphyrin Precursor 5**

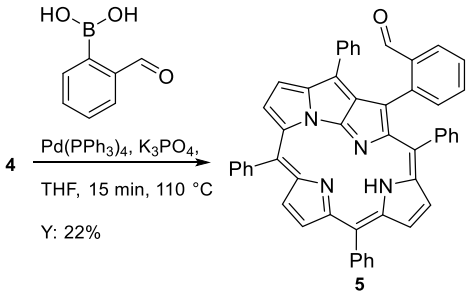


increased temperature of 110 °C and a reduced reaction time of 15 min in a pressure vial.[24] Some reported catalysts for sterically demanding Suzuki−Miyaura cross-coupling reactions were also tried, but none led to a successful reaction.[29−31] Diluted reactions or exchange of $K_3PO_4$ with $Cs_2CO_3$ resulted in slightly lowered yields. At the same time, N-fused-tetraphenyl porphyrin remained the primary side product.

The $^1$H NMR spectra of **5** showed broad signals for the pyrrolic protons, which could be narrowed by adding 1 M aqueous HCl solution in a ratio of 1:10 to reduce $\pi$-stacking aggregation.[32] The same effect could not be observed by using the analogous deuterated solvents. However, by dissolving **5** in $CD_2Cl_2$ instead of $CDCl_3$, sharper signals could be obtained.

The resulting spectrum exhibits a shifted sharp singlet at 10.16 ppm, confirming the aldehyde functionality. Furthermore, the broad singlet at 8.00 ppm can be assigned to the NH proton arising not in the upfield but in the downfield region for the N-fused derivative, in sharp contrast to regular porphyrins.

The aldehyde functionality was then applied in a subsequent condensation reaction to synthesize a dimer consisting of an NFP and a regular porphyrin monomer, the "N-fused-regular dimer" **6** (Scheme 4). We label it [3H-NFR] to highlight its three NH protons.

To a degassed solution of $CH_2Cl_2$ and formyl-phenyl-N-fused porphyrin **5**, pyrrole **1**, PhCHO, and TFA as acid catalysts were added dropwise over 19 h to guarantee a steady build-up of the dimeric ligand **6**. The progress of the reaction was constantly monitored via TLC. As soon as the conversion of the starting material slowed down, pyrrole and PhCHO were added in their respective stoichiometric ratios. We thus report a new synthetic route to the first dimeric ligand system containing an NFP and a regular porphyrin—yielding **6** in a

**Scheme 4. Mixed Condensation Reaction Yielding the First Dimeric Ligand System Containing an N-Fused Porphyrin and a Regular Porphyrin 6, [3H-NFR]**

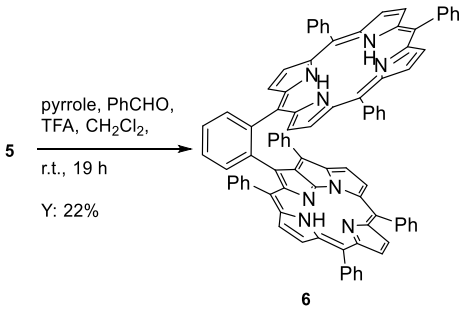


total yield of 0.77% over five steps, starting from pyrrole and PhCHO.

The $^1$H NMR spectrum again shows line broadening due to stacking effects, but this can be circumvented by adding acid or pyridine-$d_5$ as a base. In a comprehensive experimental study of N-heterocyclic $\pi$-stacking interactions of different pyridines by Shimizu et al., this effect has been discussed in depth and could be exploited here.[33] In this case, the optimal amount of added pyridine-$d_5$ was assessed by recording $^1$H NMR spectra. Figure 1 shows that the pyrrolic/aromatic and NH protons condensed into sharper signals depending on the ratio of $CD_2Cl_2$/pyridine-$d_5$. Unfortunately, changing the deuterated solvent/solvent mixture, as examined for DMF-$d_7$, DMF-$d_7$/pyridine-$d_5$ (25:1), TFA-$d_1$, and $CD_2Cl_2$/TFA-$d_1$ (25:1), did not result in sharper signals in the respective NMR spectra recorded. Besides that, tempered $^1$H NMR studies in DMF-$d_7$ at 50, 90, and 130 °C did not result in better resolved $^1$H NMR spectra, as depicted in more detail in the Supporting Information (Section S3.2.2, Figure S20). Nevertheless, the UV−vis spectrum of the dimeric ligand (Supporting Information, Section S3.2.2, Figure S21) clearly exhibits not only Q-bands in the range of 500−580 nm but also Stokes-shifted, weak Q-like bands at circa 650 and 720 nm, which can be assigned to the $S_0 \rightarrow S_1$ transition of the NFP core.

The same explanation, i.e., reduction of $\pi$-stacking, put forward above for the formyl-phenyl-N-fused porphyrin **5**, is also valid here for the $^1$H NMR spectra of the dimeric case **6**. The effect for the NH protons at −4.0 to −4.5 ppm of the regular porphyrin component is even more drastic since they experience line broadening already due to exchange effects arising from the two equivalent tautomeric forms. Furthermore, the cofacially arranged porphyrin resp. NFP subunits might contribute to intramolecular relaxation processes through space, as suggested by the DFT-calculated structure of the isolated **6** molecule in Figure 2.

As outlined above, one reason for synthesizing a ligand system containing an NFP unit covalently linked to a regular porphyrin was to bring the same two metal centers into spatial proximity but in two different oxidation states. Before documenting the proof-of-principle synthesis of such a complex, we first examine the structure of the ligand more closely. While the NMR measurements discussed above suggest that **6** in $CH_2Cl_2$ solution forms a structure with strong ring−ring interactions which become weaker upon adding pyridine-$d_5$, the NMR spectra themselves are insufficient to deduce more detailed structural parameters.

**3D Structure Elucidation in the Gas Phase.** Since it was not possible to crystallize the dimer to obtain the molecular structure in the solid, we have instead used ion mobility spectrometry (IMS) combined with mass spectrometric (MS) measurements to obtain further structural information on the corresponding singly protonated dimers in the gas phase. For this, we have followed the same procedure as already applied by us for other porphyrins and porphyrin oligomers[24,25] using a TIMS-TOFMS instrument equipped with an electrospray ionization (ESI) source (Bruker). The mode of operation of trapped IMS (TIMS), a high-resolution IMS variant, has been described elsewhere.[49] Briefly, in TIMS, ions are held in a pressure-difference induced gas stream (here: $N_2$) by an electric field, which is lowered over time. This leads to the consecutive elution of the accumulated ions as a function of their ion mobility K.[50] The resulting mobilogram is analyzed to yield an elution time which can be converted into a collision cross section (CCS, here: $^{TIMS}CCS_{N2}$) via calibration against well-known drift tube $CCS_{N2}$ values of the Agilent TuneMix published by Stow. et al.[51] An additional explanation of TIMS and the experimental parameters used in our measurements is given in the Supporting Information. The CCS of a specific molecular ion can be interpreted as its rotationally averaged interaction surface with a buffer gas (here: $N_2$);[50] hence, the more compact the structure of the ion, the smaller the CCS. With TIMS, a high-resolution variant of IMS, CCS resolution is high enough to allow a rough determination of the ring separation in the dimeric ligand system of interest here, as we will show next.

In Figure 3, we show the structures, sum formulas, and mobilograms of three different protonated porphyrin-based dimers, namely, the protonated form of the newly synthesized NFR dimer **6**, $[(3H\text{-}NFR) + H]^+$, the already published, phenylene-linked protonated BMOBBP-dimer, $[(4H\text{-}BMOBBP) + H]^+$ and $[(2H\text{-}TPP)_2 + H]^+$ a non-covalently linked protonated dimer of free-base tetraphenyl porphyrin (2H-TPP).[24] (Note that the latter dimers form on their own by ESI once the concentration of the respective monomer is sufficiently high). We label these protonated species as **7**, **8**, and **9**, respectively, also to distinguish them from their neutral congeners. Note that their sum formulas are the same except for the loss of 2 (or 4) hydrogen atoms (relative to $[(2H + TPP)_2 + H]^+$) and, therefore, that the experimental $^{TIMS}CCS_{N2}$-values can, to first order, be compared directly without the need for calculations.

It is apparent in Figure 3 that $[(2H + TPP)_2 + H]^+$ has the largest $^{TIMS}CCS_{N2}$ of the three dimers shown. In the absence of covalent links between the two subunits, isolated $[(2H + TPP)_2 + H]^+$ is held together primarily by dispersion interactions between the porphyrin rings and consequently forms a cofacially stacked dimer structure, qualitatively like that postulated for porphyrin H-aggregates in solution.[52−55] In a previous publication, we inferred that in gas-phase, the protonated BMOBBP dimer has a similar (but slightly more compact) cofacial arrangement.[24] Given that protonated NFR has an even smaller CCS, we infer that it must also be a cofacially stacked dimer and that its ring−ring separation must be smaller than in either $[(2H + TPP)_2 + H]^+$ or $[(4H\text{-}BMOBBP) + H]^+$.

However, this finding is only valid for **7** in the gas phase and not necessarily in solution. Our NMR measurements indicate some $\pi$-stacking of (neutral) **6** in $CD_2Cl_2$. It is unclear, though, how exactly the rings/molecules orient relative to each other and whether $\pi$-stacking is peculiar to this solvent. To learn

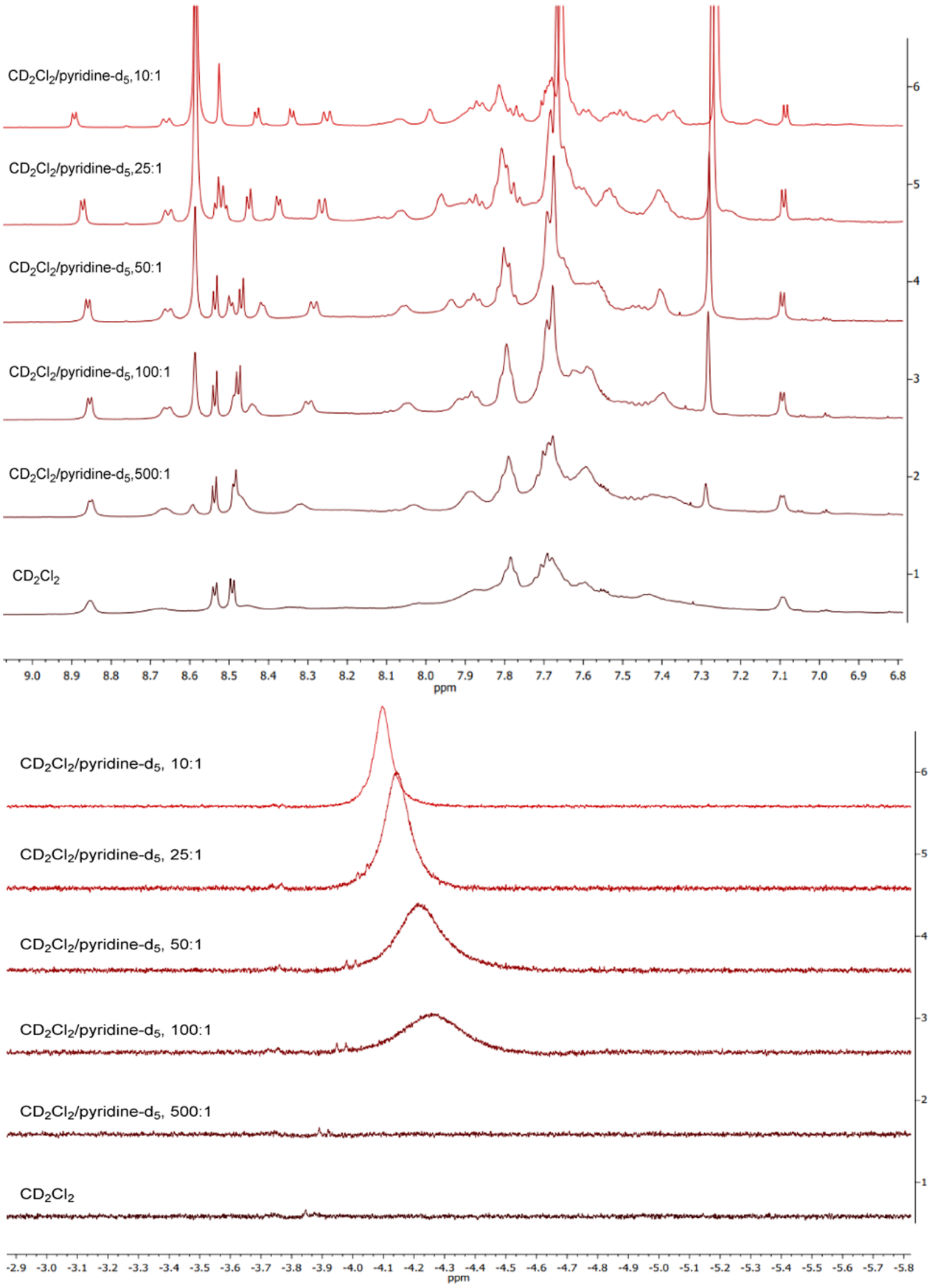


**Figure 1.** Downfield and highfield regions of the $^{1}$H NMR spectra of the cofacial ligand **6** showing the effect of the $CD_2Cl_2$/pyridine-$d_5$ ratio on signal widths. In the upper part, the resonances of the aromatic protons are shown—in the lower part, the resonances of the NH protons are displayed.

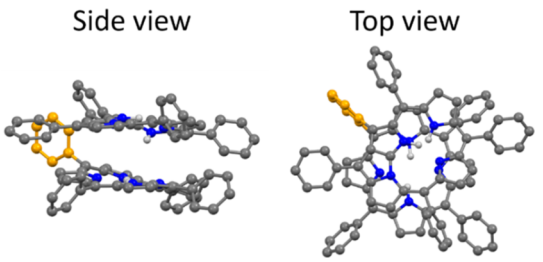


**Figure 2.** DFT-calculated structure of the protonated, dimeric ligand system in charge state +1 containing an N-fused porphyrin and a regular porphyrin, **7**, is shown in side and top views. Carbon atoms are displayed in gray and nitrogen in blue. Hydrogen atoms have been hidden except for the internal ones shown in white. The linker phenyl is displayed in orange. The calculation was carried out in Turbomole[34−36] using the basis set def2-SVP;[37−41] the functional TPSS[42−46] and the dispersion correction D3-BJ.[47,48]

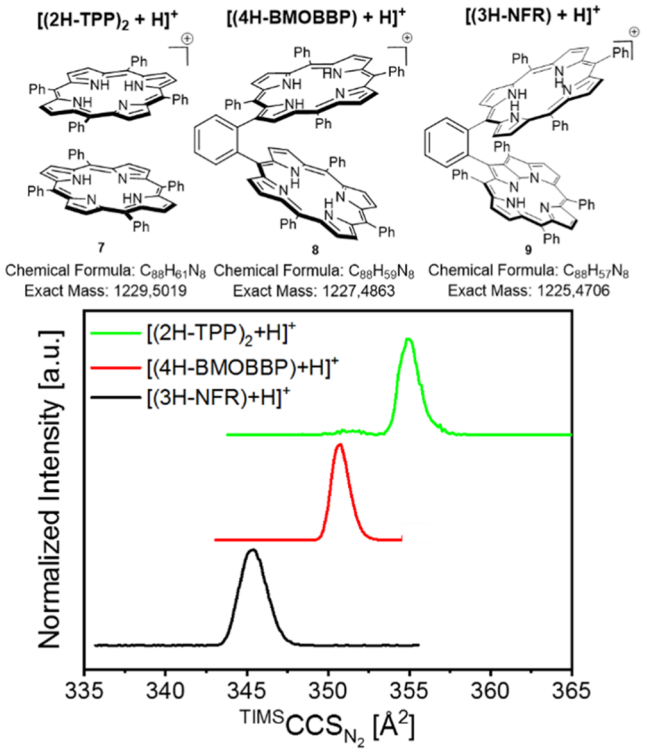


**Figure 3.** Structures, chemical formulas, masses, and mobilograms of three different protonated porphyrin-dimers, **7**−**9**, are shown. As can be seen, the cofacial dimer held together by dispersion interactions, ($[(2H\text{-}TPP)_2 + H]^+$) has the highest $^{TIMS}CCS_{N2}$. Therefore, the structures of the other dimers have to be slightly more compact than $[(2H\text{-}TPP)_2 + H]^+$, and all three dimers have a cofacially stacked structure.

more about the structure of the NFR ligand in the liquid phase, we therefore next chose a "coordination labeling" approach.

It is known in the literature that a free base NFP monomer can coordinate Mn(I)-$(CO)_3$ to form an on-top distorted tetrahedral structure with Mn(I) interacting with three of the four porphyrinic nitrogens, leading to a distorted octahedral coordination of the Mn(I).[7] When [3H-NFR] is reacted with $Mn(CO)_5Br$ in DMF, a species is formed, which is detected by ESI-MS as $[2Mn\text{-}3(CO)\text{-}NFR]^+$, **10** (see the Supporting Information for synthetic details and mass spectra).

Most likely, this comprises a Mn(I)-$(CO)_3$ unit bound to the NFP and a Mn(III) complexed with the regular porphyrin. This is supported by the presence of small amounts of $[Mn\text{-}H\text{-}NFR]^+$ (i.e., a complex with Mn(III) bound to the porphyrin together with an empty NFP site) in the corresponding ESI mass spectrum (see also Supporting Information). Two different isomers of such a $[2Mn\text{-}3(CO)\text{-}NFR]^+$ species would be possible: (i) $(CO)_3$-Mn(I) is "internally" coordinated to the NFP and thus held between the two porphyrinic units, or (ii) $(CO)_3$-Mn(I) is "externally" attached to the NFP. The respective theoretical structures are shown in Figure 4.

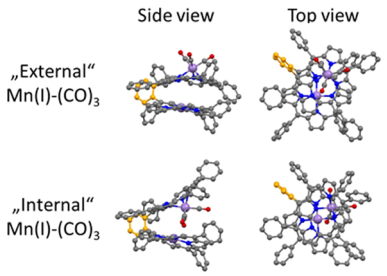


**Figure 4.** DFT-calculated structure of the Mn(I)Mn(III) complex **10**, presented in side view and top view, as a model for $[2Mn\text{-}3(CO)\text{-}NFR]^+$. The calculations were carried out in Turbomole with def2-SVP, TPSS, and D3-BJ. The carbon atoms are shown in gray (with an orange linker-phenyl for clarity), the nitrogen atoms are plotted in light blue, the oxygen atoms are plotted in red, and the manganese atoms are plotted in purple. They represent the structures in their respective lowest-energy quintet configurations. The relative energies and theoretical CCS values are shown in Table 1.

Assuming the NFR ligand is again cofacially bound in DMF (similar to the situation inferred for $CD_2Cl_2$ solutions), the reaction to form the external isomer can proceed without steric hindrance, whereas the internal isomer requires substantial activation energy to open the "clam shell". We therefore expect $[2Mn\text{-}3(CO)\text{-}NFR]^+$ to exist in only one "external" isomeric form. To test this, we conducted a TIMS measurement of the $[2Mn\text{-}3(CO)\text{-}NFR]^+$ complex. The corresponding mobilogram is shown in Figure 5. It consists of only one peak. This can mean that (i) only one isomer is present, (ii) multiple isomers are indistinguishable in terms of their CCS even in the highly resolved TIMS measurement, or (iii) nominally distinguishable isomers rapidly interconvert on the experimental timescale.[56] The latter seems unlikely since interconversion between an external and internal isomer would

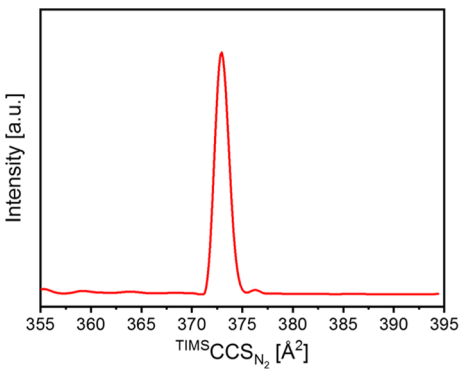


**Figure 5.** High-resolution mobilogram of $[2Mn\text{-}3(CO)\text{-}NFR]^+$. See the Supporting Information for further details.

require dramatic rearrangements incompatible with the vibrational temperatures accessed.

To explore whether TIMS would in fact allow us to resolve an external from an internal isomer if both were present, we have performed DFT calculations on both dimanganese complexes with Turbomole using the basis set def2-SVP; the functional TPSS and the dispersion correction D3-BJ. Since Mn(III) and Mn(I) are open-shell, one has to consider different possible spin-states of the [2Mn-3(CO)-NFR]+ ion. The relative energies of both isomers in five different spin states are given in Table 1. For both structures, the quintet state is lowest in energy, with a gap of roughly 0.6 eV to the second lowest spin state (triplet). Based upon these structures and their calculated Mulliken charges, we used the trajectory method (TM)[57,58] in IMoS (Version 1.09)[59,60] to predict the corresponding theoretical CCS values (for details, see the Supporting Information, and for results see Table 1). The $CCS_{N2}$ values of the "external" and "internal" isomers (depending on the spin state) are 377−379 and 389−394 Å$^2$, respectively, i.e., a difference of ca. 10−17 Å$^2$, which would be well resolvable by TIMS, which has a typical CCS resolution, CCS/ΔCCS of >200 for ions of this kind. Therefore, the existence of a second isomer can be ruled out. Since we already ruled out interconversion between the "internal" and the "external" isomers, we conclude that NFR is arranged in a closed stack in the liquid phase, and the existing isomer is the external one.

**Table 1. Energies and Predicted CCS Values of DFT-Calculated Internal and External Isomers of Complex 10 (See Also Figure 4)[a]**

| spin state | rel. energy of the "external" isomer (in eV) | $^{TM}CCS_{N2}$ of the "external" isomer (in Å$^2$) | rel. energy of the "internal" isomer (in eV) | $^{TM}CCS_{N2}$ of the "internal" isomer (in Å$^2$) |
|---|---|---|---|---|
| singlet | 2.2 | 378 | 2.5 | 392 |
| triplet | 0.6 | 378 | 0.7 | 391 |
| quintet | 0.0 | 378 | 0.1 | 392 |
| septet | 0.9 | 379 | 1.0 | 394 |
| nonet | 2.1 | 377 | 2.4 | 389 |

[a]The calculations were carried out in Turbomole with def2-SVP, TPSS, and D3-BJ. The quintets are the lowest in energy, but the two isomers are only 0.1 eV apart and can only be distinguished on the basis of their predicted collision cross sections ($CCS_{N2}$, see also Supporting Information).

## CONCLUSIONS

We present a straightforward new synthesis route for a dimeric ligand system containing an N-fused porphyrin and a regular porphyrin **6**, starting from pyrrole and benzaldehyde. The ligand was obtained in an overall yield of 0.77% via 5 steps. DFT calculations on the isolated molecule predict it to consist of a cofacial, $\pi$-stacked arrangement of the two porphyrinic rings. To explore this experimentally, ion mobility measurements were performed on protonated **6**, indicating an even smaller collision cross-section than for the protonated, non-covalently linked free-base TPP dimer, which forms a compact cofacial structure in the gas phase (Hiroyuki Furuta). To confirm that 6 also has a cofacial structure in solution, we performed $^1$H NMR studies in $CD_2Cl_2$/pyridine-$d_5$ solvent mixtures. Additionally, we reacted **6** with $Mn(CO)_5Br$ in DMF to yield a dimanganese product detectable by ESI-MS as [2Mn-3(CO)-NFR]$^+$. Ion mobility shows this to comprise only one of two possible isomers, as expected for cofacial **6**. Thus, our dimeric ligand system containing NFP and a regular free-base porphyrin allows us to stabilize two manganese atoms in different oxidation states ($(CO)_3$-Mn(I) to NFP and Mn(III) to the free-base porphyrin).

## ASSOCIATED CONTENT

### Supporting Information

The Supporting Information is available free of charge at https://pubs.acs.org/doi/10.1021/acs.organomet.3c00116.

Experimental procedures and spectral data for all the new compounds (PDF)
[3H-NFR+H]+ (XYZ)
[2Mn-3(CO)-NFR]+ - External Isomer in Quintett-state (XYZ)
[2Mn-3(CO)-NFR]+ - Internal Isomer in Quintett-state (XYZ)

## AUTHOR INFORMATION


### Corresponding Authors

**Manfred M. Kappes** − *Institute of Physical Chemistry, Karlsruhe Institute of Technology (KIT), 76131 Karlsruhe, Germany; Institute of Nanotechnology, Karlsruhe Institute of Technology (KIT), D-76344 Eggenstein-Leopoldshafen, Germany;* orcid.org/0000-0002-1199-1730; Phone: (+49)-721- 608-42094; Email: manfred.kappes@kit.edu; Fax: (+49)-721-608-47232

**Stefan Bräse** − *Institute of Organic Chemistry, Karlsruhe Institute of Technology (KIT), 76131 Karlsruhe, Germany; Institute of Biological and Chemical Systems−Functional Molecular Systems (IBCS-FMS), Karlsruhe Institute of Technology (KIT), D 76344 Eggenstein-Leopoldshafen, Germany;* orcid.org/0000-0003-4845-3191; Phone: (+49)-721-608-42903; Email: braese@kit.edu; Fax: (+49)-721-608-48581

### Authors

**Christoph Schissler** − *Institute of Organic Chemistry, Karlsruhe Institute of Technology (KIT), 76131 Karlsruhe, Germany*

**Erik K. Schneider** − *Institute of Physical Chemistry, Karlsruhe Institute of Technology (KIT), 76131 Karlsruhe, Germany*

**Michael Rotter** − *Institute of Organic Chemistry, Karlsruhe Institute of Technology (KIT), 76131 Karlsruhe, Germany*

**Silke Notter** − *Institute of Inorganic Chemistry, Karlsruhe Institute for Technology (KIT), 76131 Karlsruhe, Germany*

**Carsten Geier** − *Institute of Organic Chemistry, Karlsruhe Institute of Technology (KIT), 76131 Karlsruhe, Germany*

**Patrick Weis** − *Institute of Physical Chemistry, Karlsruhe Institute of Technology (KIT), 76131 Karlsruhe, Germany;* orcid.org/0000-0001-7006-6759


### Notes

The authors declare no competing financial interest.

## ACKNOWLEDGMENTS


We thank S. Jaschik, F. Bösch, C. Schoch, and C. Geier [Karlsruhe Institute of Technology (KIT)] for their help in conducting the synthesis of the precursors. C.S. gratefully

acknowledges the Fonds der Chemischen Industrie (FCI) and the graduate program of the federal state of Baden-Württemberg (LGF) for financial support. S.B. also thanks the Collaborative Research Centre TRR 88 "3MET" and the Deutsche Forschungsgemeinschaft (DFG, German Research Foundation) for support through project B2. Additionally, S.B. acknowledges support under Germany's Excellence Strategy via the Excellence Cluster 3D Matter Made to Order (EXC-2082/1-390761711). E.K.S., P.W., and M.M.K. gratefully acknowledge support by the DFG, as administered by the Collaborative Research Centre TRR 88 "3MET" through project C6. M.M.K. thanks KIT for funding the TIMS-TOFMS used in this study.

## REFERENCES

(1) Senge, M. O. Stirring the porphyrin alphabet soup—functionalization reactions for porphyrins. *Chem. Commun.* **2011**, *47*, 1943−1960.
(2) Yamamoto, T.; Abraham, J. A.; Mori, S.; Toganoh, M.; Shimizu, S.; Ishida, M.; Furuta, H. Tungsten (VI) Complex of N-Fused Porphyrin Absorbing Near-Infrared Light beyond 1000 nm. *Chem.—Asian J.* **2020**, *15*, 748−752.
(3) Fabian, J.; Nakazumi, H.; Matsuoka, M. Near-infrared absorbing dyes. *Chem. Rev.* **1992**, *92*, 1197−1226.
(4) Furuta, H.; Ishizuka, T.; Osuka, A.; Ogawa, T. N-Fused Porphyrin": A New Tetrapyrrolic Porphyrinoid with a Fused Tripentacyclic Ring. *J. Am. Chem. Soc.* **2000**, *122*, 5748−5757.
(5) Młodzianowska, A.; Latos-Grażyński, L.; Szterenberg, L.; Stępień, M. Single-boron complexes of N-confused and N-fused porphyrins. *Inorg. Chem.* **2007**, *46*, 6950−6957.
(6) Młodzianowska, A.; Latos-Grażyński, L.; Szterenberg, L. Phosphorus complexes of N-fused porphyrin and its reduced derivatives: new isomers of porphyrin stabilized via coordination. *Inorg. Chem.* **2008**, *47*, 6364−6374.
(7) Ikeda, S.; Toganoh, M.; Furuta, H. Synthesis, Reactivity, and Properties of N-Fused Porphyrin Manganese(I) Tricarbonyl Complexes. *Inorg. Chem.* **2011**, *50*, 6029−6043.
(8) Yamamoto, T.; Abraham, J. A.; Mori, S.; Toganoh, M.; Shimizu, S.; Ishida, M.; Furuta, H. Tungsten (VI) Complex of N-Fused Porphyrin Absorbing Near-Infrared Light beyond 1000 nm. *Chem.—Asian J.* **2020**, *15*, 748−752.
(9) Toganoh, M.; Ishizuka, T.; Furuta, H. Synthesis and properties of rhenium tricarbonyl complex bearing N-fused tetraphenylporphyrin ligand. *Chem. Commun.* **2004**, *21*, 2464−2465.
(10) Ishizuka, T.; Ikeda, S.; Toganoh, M.; Yoshida, I.; Ishikawa, Y.; Osuka, A.; Furuta, H. Substitution, dimerization, metalation, and ring-opening reactions of N-fused porphyrins. *Tetrahedron Lett.* **2008**, *64*, 4037−4050.
(11) Abraham, J. A.; Mori, S.; Ishida, M.; Furuta, H. Synthesis and Characterization of N-Fused Porphyrin Rhodium Complex with an Isomerized Cyclooctadiene Ligand. *Chem. Lett.* **2021**, *50*, 1707−1709.
(12) Arnold, D. P.; Blok, J. The coordination chemistry of tin porphyrin complexes. *Coord. Chem. Rev.* **2004**, *248*, 299−319.
(13) Boitrel, B.; Halime, Z.; Michaudet, L.; Lachkar, M.; Toupet, L. Structural characterisation of the first mononuclear bismuth porphyrin. *Chem. Commun.* **2003**, *21*, 2670−2671.
(14) Che, C.-M.; Huang, J.-S. Ruthenium and osmium porphyrin carbene complexes: synthesis, structure, and connection to the metal-mediated cyclopropanation of alkenes. *Coord. Chem. Rev.* **2002**, *231*, 151−164.
(15) Majumder, S.; Borah, B. P.; Bhuyan, J. Rhenium in the core of porphyrin and rhenium bound to the periphery of porphyrin: synthesis and applications. *Dalton Trans.* **2020**, *49*, 8419−8432.
(16) Plater, M. J.; Aiken, S.; Gelbrich, T.; Hursthouse, M. B.; Bourhill, G. Structures of Pb (II) porphyrins:[5, 10, 15, 20-tetrakis-triisopropylsilylethynylporphinato] lead (II) and [5, 15-bis-(3, 5-bis-tert-butylphenyl)-10, 20-bis-triisopropylsilylethynylporphinato] lead (II). *Polyhedron* **2001**, *20*, 3219−3224.
(17) Gross, T.; Chevalier, F.; Lindsey, J. S. Investigation of rational syntheses of heteroleptic porphyrinic lanthanide (europium, cerium) triple-decker sandwich complexes. *Inorg. Chem.* **2001**, *40*, 4762−4774.
(18) Wong, W.-K.; Zhu, X.; Wong, W.-Y. Synthesis, structure, reactivity and photoluminescence of lanthanide (III) monoporphyrinate complexes. *Coord. Chem. Rev.* **2007**, *251*, 2386−2399.
(19) Feltham, H. L.; Brooker, S. Review of purely 4f and mixed-metal nd-4f single-molecule magnets containing only one lanthanide ion. *Coord. Chem. Rev.* **2014**, *276*, 1−33.
(20) Furuta, H.; Asano, T.; Ogawa, T. N-Confused Porphyrin: A New Isomer of Tetraphenylporphyrin. *J. Am. Chem. Soc.* **1994**, *116*, 767−768.
(21) Chmielewski, P. J.; Latos-Grażyński, L.; Rachlewicz, K.; Glowiak, T. Tetra-p-tolylporphyrin with an Inverted Pyrrole Ring: A Novel Isomer of Porphyrin. *Angew. Chem., Int. Ed.* **1994**, *33*, 779−781.
(22) Toganoh, M.; Furuta, H. N-Fused Porphyrin: A Maverick Member of the Porphyrin Family. *Chem. Lett.* **2019**, *48*, 615−622.
(23) Senge, M. O. Extroverted Confusion—Linus Pauling, Melvin Calvin, and Porphyrin Isomers. *Angew. Chem., Int. Ed.* **2011**, *50*, 4272−4277.
(24) Schissler, C.; Schneider, E. K.; Felker, B.; Weis, P.; Nieger, M.; Kappes, M. M.; Bräse, S. A Synthetic Strategy for Cofacial Porphyrin-Based Homo-and Heterobimetallic Complexes. *Chem.—Eur. J.* **2021**, *27*, 3047−3054.
(25) Schissler, C.; Schneider, E. K.; Lebedkin, S.; Weis, P.; Niedner-Schatteburg, G.; Kappes, M. M.; Bräse, S. Novel Cofacial Porphyrin-Based Homo-and Heterotrimetallic Complexes of Transition Metals. *Chem.—Eur. J.* **2021**, *27*, 15202−15208.
(26) Geier, G. R.; Haynes, D. M.; Lindsey, J. S. An efficient one-flask synthesis of N-confused tetraphenylporphyrin. *Org. Lett.* **1999**, *1*, 1455−1458.
(27) Furuta, H.; Ishizuka, T.; Osuka, A.; Dejima, H.; Nakagawa, H.; Ishikawa, Y. NH tautomerism of N-confused porphyrin. *J. Am. Chem. Soc.* **2001**, *123*, 6207−6208.
(28) Furuta, H.; Maeda, H.; Osuka, A. Theoretical study of stability, structures, and aromaticity of multiply N-confused porphyrins. *J. Org. Chem.* **2001**, *66*, 8563−8572.
(29) Billingsley, K.; Buchwald, S. L. Highly efficient monophosphine-based catalyst for the palladium-catalyzed suzuki− miyaura reaction of heteroaryl halides and heteroaryl boronic acids and esters. *J. Am. Chem. Soc.* **2007**, *129*, 3358−3366.
(30) Miura, M. Rational ligand design in constructing efficient catalyst systems for Suzuki−Miyaura coupling. *Angew. Chem., Int. Ed.* **2004**, *43*, 2201−2203.
(31) Zhao, Q.; Li, C.; Senanayake, C. H.; Tang, W. An efficient method for sterically demanding Suzuki−Miyaura coupling reactions. *Chem.—Eur. J.* **2013**, *19*, 2261−2265.
(32) Andrianov, D.; Rybakov, V.; Cheprakov, A. Between porphyrins and phthalocyanines: 10, 20-diaryl-5, 15-tetrabenzodiazaporphyrins. *Chem. Commun.* **2014**, *50*, 7953−7955.
(33) Li, P.; Zhao, C.; Smith, M. D.; Shimizu, K. D. Comprehensive experimental study of N-heterocyclic $\pi$-stacking interactions of neutral and cationic pyridines. *J. Org. Chem.* **2013**, *78*, 5303−5313.
(34) Ahlrichs, R.; Bär, M.; Häser, M.; Horn, H.; Kölmel, C. Electronic structure calculations on workstation computers: The program system turbomole. *Chem. Phys. Lett.* **1989**, *162*, 165−169.
(35) Balasubramani, S. G.; Chen, G. P.; Coriani, S.; Diedenhofen, M.; Frank, M. S.; Franzke, Y. J.; Furche, F.; Grotjahn, R.; Harding, M. E.; Hättig, C.; et al. TURBOMOLE: Modular program suite for ab initio quantum-chemical and condensed-matter simulations. *Chem. Phys. Phys. Chem.* **2020**, *152*, 184107.
(36) Furche, F.; Ahlrichs, R.; Hättig, C.; Klopper, W.; Sierka, M.; Weigend, F. *TURBOMOLE V7. 5.1 2021, a Development of University of Karlsruhe and Forschungszentrum Karlsruhe GmbH, 1989−2007*; TURBOMOLE GmbH, 2007. https://www.turbomole.org/.

(37) Eichkorn, K.; Treutler, O.; Öhm, H.; Häser, M.; Ahlrichs, R. Auxiliary basis sets to approximate Coulomb potentials. *Chem. Phys. Lett.* **1995**, *240*, 283−290.
(38) Weigend, F. Accurate Coulomb-Fitting Basis Sets for H to Rn. *Phys. Chem. Chem. Phys.* **2006**, *8*, 1057−1065.
(39) Weigend, F.; Ahlrichs, R. Balanced Basis Sets of Split Valence, Triple Zeta Valence And Quadruple Zeta Valence Quality For H to Rn: Design And Assessment of Accuracy. *Phys. Chem. Chem. Phys.* **2005**, *7*, 3297−3305.
(40) Weigend, F.; Häser, M.; Patzelt, H.; Ahlrichs, R. RI-MP2: optimized auxiliary basis sets and demonstration of efficiency. *Chem. Phys. Lett.* **1998**, *294*, 143−152.
(41) Schäfer, A.; Horn, H.; Ahlrichs, R. Fully optimized contracted Gaussian basis sets for atoms Li to Kr. *J. Phys. Chem.* **1992**, *97*, 2571−2577.
(42) Slater, J. C. A Simplification of The Hartree-Fock Method. *Phys. Rev.* **1951**, *81*, 385−390.
(43) Dirac, P. A. M. The quantum theory of the electron. *Proc. Math. Phys.* **1928**, *117*, 610−624.
(44) Perdew, J. P.; Wang, Y. Pair-distribution function and its coupling-constant average for the spin-polarized electron gas. *Phys. Rev. B: Condens. Matter Mater. Phys.* **1992**, *46*, 12947−12954.
(45) Perdew, J. P.; Wang, Y. Erratum: Accurate and simple analytic representation of the electron-gas correlation energy [Phys. Rev. B 45, 13244 (1992)]. *Phys. Rev. B* **2018**, *98*, 079904.
(46) Tao, J.; Perdew, J. P.; Staroverov, V. N.; Scuseria, G. E. Climbing the density functional ladder: Nonempirical meta−generalized gradient approximation designed for molecules and solids. *Phys. Rev. Lett.* **2003**, *91*, 146401.
(47) Grimme, S.; Antony, J.; Ehrlich, S.; Krieg, H. A consistent and accurate ab initio parametrization of density functional dispersion correction (DFT-D) for the 94 elements H-Pu. *J. Chem. Phys.* **2010**, *132*, 154104.
(48) Grimme, S.; Ehrlich, S.; Goerigk, L. Effect of the damping function in dispersion corrected density functional theory. *J. Comput. Chem.* **2011**, *32*, 1456−1465.
(49) Michelmann, K.; Silveira, J. A.; Ridgeway, M. E.; Park, M. A. Fundamentals of Trapped Ion Mobility Spectrometry. *J. Am. Soc. Mass Spectrom.* **2014**, *26*, 14−24.
(50) Revercomb, H.; Mason, E. A. Theory of Plasma Chromatography/Gaseous Electrophoresis. Review. *Anal. Chem.* **1975**, *47*, 970−983.
(51) Stow, S. M.; Causon, T. J.; Zheng, X.; Kurulugama, R. T.; Mairinger, T.; May, J. C.; Rennie, E. E.; Baker, E. S.; Smith, R. D.; McLean, J. A.; et al. An Interlaboratory Evaluation of Drift Tube Ion Mobility−Mass Spectrometry Collision Cross Section Measurements. *Anal. Chem.* **2017**, *89*, 9048−9055.
(52) Pescitelli, G.; Di Bari, L.; Berova, N. Application of electronic circular dichroism in the study of supramolecular systems. *Chem. Soc. Rev.* **2014**, *43*, 5211−5233.
(53) Maiti, N. C.; Mazumdar, S.; Periasamy, N. J-and H-aggregates of porphyrin− surfactant complexes: time-resolved fluorescence and other spectroscopic studies. *J. Phys. Chem. B* **1998**, *102*, 1528−1538.
(54) Brendle, K.; Schwarz, U.; Jäger, P.; Weis, P.; Kappes, M. Structures of Metalloporphyrin−Oligomer Multianions: Cofacial versus Coplanar Motifs as Resolved by Ion Mobility Spectrometry. *J. Phys. Chem. A* **2016**, *120*, 8716−8724.
(55) Jäger, P.; Brendle, K.; Schneider, E.; Kohaut, S.; Armbruster, M. K.; Fink, K.; Weis, P.; Kappes, M. M. Photodissociation of Free Metalloporphyrin Dimer Multianions. *J. Phys. Chem. A* **2018**, *122*, 2974−2982.
(56) Poyer, S.; Comby-Zerbino, C.; Choi, C. M.; MacAleese, L.; Deo, C.; Bogliotti, N.; Xie, J.; Salpin, J.-Y.; Dugourd, P.; Chirot, F. Conformational dynamics in ion mobility data. *Anal. Chem.* **2017**, *89*, 4230−4237.
(57) Mesleh, M.; Hunter, J.; Shvartsburg, A.; Schatz, G. C.; Jarrold, M. Structural information from ion mobility measurements: effects of the long-range potential. *J. Phys. Chem. A* **1996**, *100*, 16082−16086.
(58) Mesleh, M.; Hunter, J.; Shvartsburg, A.; Schatz, G.; Jarrold, M. Structural information from ion mobility measurements: effects of the long-range potential. *J. Phys. Chem. A* **1997**, *101*, 968.
(59) Larriba, C.; Hogan, C. J., Jr Ion Mobilities in Diatomic Gases: Measurement Versus Prediction With Non-Specular Scattering Models. *J. Phys. Chem. A* **2013**, *117*, 3887−3901.
(60) Wu, T.; Derrick, J.; Nahin, M.; Chen, X.; Larriba-Andaluz, C. Optimization of Long Range Potential Interaction Parameters in Ion Mobility Spectrometry. *J. Chem. Phys.* **2018**, *148*, 074102.